

ORIGINAL**Age-dependent texture features in skeletal muscle ultrasonography**

Hiroyuki Nodera¹, Kazuki Sogawa², Naoko Takamatsu^{1,3}, Atsuko Mori¹, Hiroki Yamazaki¹, Yuishin Izumi^{1,3}, and Ryuji Kaji¹

¹Department of Neurology, Tokushima University, Tokushima, Japan, ²Tokushima University, Faculty of Medicine, Tokushima, Japan, ³Vihara Hananosato Hospital, Hiroshima, Japan

Abstract : Texture analysis characterizes regions in an image by their texture content and has been utilized to infer the underlying structures of medical images such as skeletal muscles. Although potentially useful in tissue diagnosis and assessing disease progression of neuromuscular diseases, the use of texture analysis in such purposes are limited, due to lack of information such as effects of aging. Thus, we performed texture analysis of medial gastrocnemius in healthy individuals from their 20s to late 80s. Among the 283 texture features in 6 classes, the features related to histogram, co-occurrence matrix, absolute gradient, and wavelet were correlated to age in 17-40% of the parameters, while none of the features related to run-length matrix and autoregressive model had significant correlation to age. This study showed that age-dependency in many texture features are present and need to be taken into account in elucidating the clinical significance. By contrast, the features related to run-length matrix and autoregressive model could have clinical utility. *J. Med. Invest.* 65 : 274-279, August, 2018

Keywords : skeletal muscle, ultrasound, texture, run-length matrix, autoregressive model

INTRODUCTION

Muscle ultrasound is a non-invasive imaging technique that detects histological abnormalities as seen in various neuromuscular diseases, both neurogenic and myogenic in nature (1). In order to avoid subjective bias, muscle images have been assessed quantitatively, employing parameters such as thickness, echo intensities, and a pennation angle, all of which eventually reflect macroscopic observation (2). On the other hand, texture analysis can be regarded as a microscopic view of images, by quantifying intuitive qualities described as rough, smooth, or bumpy as a function of spatial variation in neighboring pixel intensities (3). Various texture analysis features have been widely utilized in different imaging modalities, such as CT, MRI, mammography, and PET (3, 4). By quantifying a target tissue, characteristic texture features could directly connect imaging characteristics and underlying pathology, thus become an integral component of a modern concept of radiomics (5).

Texture analysis of skeletal muscle ultrasound has potential clinical implications in neuromuscular diseases. For instance, Sogawa and colleagues recently reported that texture analysis of muscle ultrasound can distinguish patients with myogenic and neurogenic diseases, thus texture analysis could be a useful technique to assess underlying muscle pathology (6). Nevertheless, detailed information in muscle texture features is yet fully available and clinical application of texture analysis should be based on careful evaluation of texture parameters, including potential age-dependency. Therefore, the aim of the present study was to assess potential age-dependency of texture features of skeletal muscle

ultrasound images.

METHODS*Inclusion criteria of the subjects*

The study was approved by the Institutional Review Board of Vihara Hananosato Hospital and Tokushima University. The subjects gave written informed consent at the time of the testing. Asymptomatic control subjects were recruited and prospectively assessed that he/she had no neurological symptom or sign. Specifically, an individual who reported symptoms suggesting cervical radiculopathy (e.g., neck pain, radicular pain, a history of whiplash injury), and peripheral nerve dysfunction as well as having medical history suggestive of potential neurogenic and myopathic conditions (e.g., diabetes mellitus, previous use of substances and drugs that are known to affect the neuromuscular system) were excluded.

Muscle ultrasound

A single sonographer (N.T.) performed sonography using a LOGIQ7 ultrasound machine (GE Healthcare) with a fixed 11-MHz linear-array transducer. Subjects were tested in the supine position, and their right medial gastrocnemius muscles were studied. The muscle was selected to because it could be affected by both neurogenic and myogenic disorders. The images obtained were saved as a bitmap format and assessed offline as described in the following paragraph.

Abbreviations :
AR = autoregressive

Received for publication March 20, 2018 ; accepted August 9, 2018.

Address correspondence and reprint requests to Hiroyuki Nodera, MD, Department of Neurology, 3-18-15 Kuramotocho, Tokushima City, 770-8503 Japan and Fax : +81-88-633-7208.

Texture analysis

Calculation of texture features was performed using the MaZda program, version 4.6 (Technical University of Lodz, Institute of Electronics, Poland). A single author (K.S., with 6 months of analyzing experience), who was blinded to the clinical information (e.g., name, age, gender), performed the texture analysis. For each subject, an eclipse-shaped ROI that covered the largest area of the gastrocnemius muscle and did not include the epimysium was selected. The ROI size ranged from 23,000 to 92,100 pixels, depending on the volume of the muscle. The MaZda program yields the following 283 parameters : histogram-derived parameters, absolute gradient (spatial variation of gray-level values), run-length matrix (counts of pixel runs with the specified gray-scale value and length in a given direction), co-occurrence matrix (information about the distribution of pairs of pixels separated by given distance and direction), autoregressive (AR) model (description of correlation between neighboring pixels), and wavelets (decomposition image frequency at different scales) (7).

In order to identify texture parameters that are prone to ages, two “attribute selection” strategies were applied in three equally divided groups of subjects according to the age of the subjects. In order to avoid duplicate analysis, the number of texture parameters were reduced by limiting the direction and distance of two pixels to the horizontally adjacent ones. For example, co-occurrence matrix was calculated at five angles (0°, 45°, 90°, 135°, and 180°) between pixels that are 1, 2, 3, 4, or 5 pixels away to each other. In case of run-length matrix-related parameters, only parameters calculating horizontally were selected. Thus, a total of 39 texture parameters out of 283 were analyzed by the following two evaluating methods using the Weka machine learning software (version 3.8.0, University of Waikato, NZ). (1) “CorrelationAttributeEval” evaluates the worth of an attribute by measuring the correlation (Pearson’s) between it and the class. (2) The OneR classifier evaluates the worth of an attribute (“OneRAttributeEval”). Attributes are ranked by the square of the weight assigned by support vector machine. Attribute selection for multiclass problems is handled by ranking attributes for each class separately using a one-vs-all

method and then “dealing” from the top of each pile to give a final ranking.

Data analysis

SPSS version 20.0J (Tokyo, Japan) was used for statistical analysis. A statistically significant *P* value was set at 0.01 due to the large number of texture parameters.

RESULTS

The demographics of the subjects are shown in the Table 1. The age distributions of women and men were similar, whereas the body mass index was greater in men than in women. The both gender groups had negative correlation between the age and height (*P* = 0.016 (combined), *P* = 0.002 in both women and men), but there was no correlation between the age vs. weight or bone mass index in either gender. The representative sonographic images from representative subjects are shown in Figure 1. As the histograms show, the mean signal intensity of the younger subject

Table 1 : characteristics of the subjects

Number	42
Gender	24 women, 18 men
Age	21–88 (years) (women : 56.5 ± 24.7 ; range 21–88 men : 55.6 ± 19.9 ; range 21–83) <i>P</i> = 0.44
Height	160.8 ± 9.4 (cm) (women 155.3 ± 6.6 ; range 140–168 men 168.3 ± 6.9 ; range 157–183) <i>P</i> < 0.001
Weight	58.4 ± 13.0 (kg) (women 49.8 ± 6.3 ; range 37–62 men 69.9 ± 10.0 ; range 50–89) <i>P</i> < 0.001
Body mass index (BMI)	22.4 ± 3.3 (women 20.6 ± 1.8 ; range 17.4–25.7 men 24.7 ± 3.4 ; range 20.3–33.1) <i>P</i> < 0.001

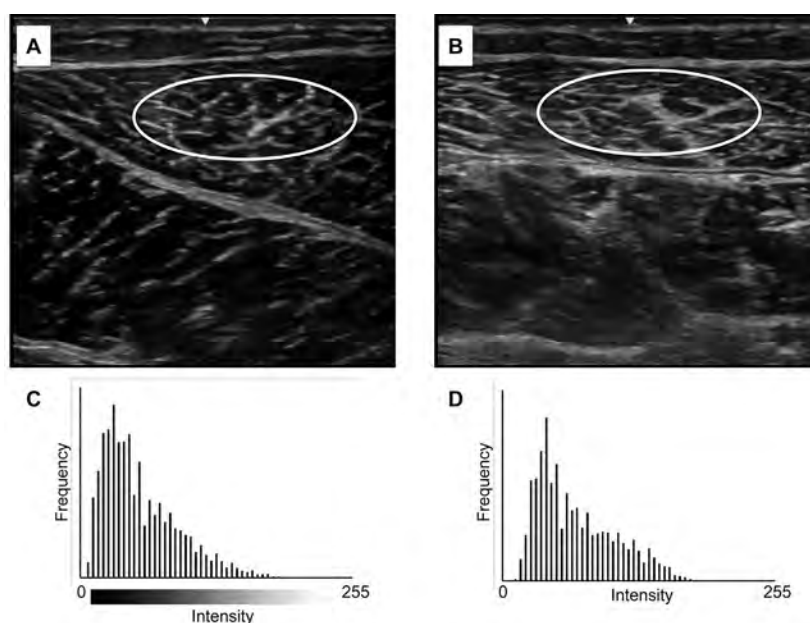


Figure 1 : Representative sonographic images of medial gastrocnemius muscle and the regions of interest (ROIs : oval) in a 24-year-old man (Panel A) and a 76-year-old man (Panel B). The distributions of signal intensities are plotted in histograms. The mean signal intensity of the older subject was slightly greater than the younger, but the standard deviations were comparable (50.3 ± 35.0 (Panel A) vs. 71.4 ± 37.3 (Panel B)).

(a 24-year-old man) was slightly lower than the older subject (a 76-year-old man), but the standard deviations were similar, thus the distinction of the images was not straightforward by the histogram alone. The representative ultrasound image and its ROI (Figure 2 A), its histogram (Figure 2B), and the texture features (Figure 2C) are shown.

Because texture parameters have been reported to be different between genders⁸, texture parameters were first compared between those in men and women (Table 2). At the significant P

value at 0.01, 13/283 texture parameters (4.6%) respectively showed significant differences between the genders. Among the six texture classes, no class showed significant difference from others in terms of the frequencies of having significant P values. However, histogram, co-occurrence matrix, and AR model tended to show higher frequencies of significant gender difference than others.

Correlation between the age and a texture parameter was then studied (Table 3). At the significant P levels at 0.01, 45/283 (15.9%) texture parameters respectively showed significant correlations



Figure 2 : The representative analysis by the MaZda software is shown. An ultrasound image of the medial gastrocnemius and its ROI is shown in Figure 2A. The histogram of grayscale is shown in Figure 2B, while and the representative texture features are shown in Figure 2C.

Table 2 : Comparison of the texture parameters between men and women

	Number of parameters	$P < 0.01$
Histogram (1)	9	1 (11%)
Co-occurrence matrix (2)	220	12 (5%)
Run-length matrix (3)	20	0 (0%)
Absolute gradient (4)	5	0 (0%)
AR model (5)	5	0 (0%)
Wavelet (6)	24	0 (0%)

Table 3 : Correlation of normalized texture parameters and normalized age (Spearman's correlation coefficient). T=total (women and men), W= women, M=men

	Number of parameters	$P < 0.01$
Histogram (1)	9	2 (22%) : T 0 (0%) : W 1 (11%) : M
Co-occurrence matrix (2)	220	37 (17%) : T 40 (18%) : W 0 (0%) : M
Run-length matrix (3)	20	0 (0%) : T,W,M
Absolute gradient (4)	5	2 (40%) : T 2 (40%) : W 0 (0%) : M
AR model (5)	5	0 (0%) : T,W,M
Wavelet (6)	24	4 (17%) : T 3 (13%) : W 0 (0%) : M

with the age. Notably, such correlation was not strong in men (1/283 texture feature showed significant correlation), whereas women had the same frequency of correlation (45/283) ($P < 0.0001$: Fisher's exact test). Among the six texture classes, the texture parameters related to run-length-matrix and AR model showed no significant correlation with the age. By contrast, absolute gradient and wavelet-related texture features showed frequent correlations with age, followed by histogram and co-occurrence matrix (Figure 3).

In order to identify factors to discriminate 3 groups of different ages, 39 representative texture features were selected (Table 4). Again, the texture features belonging to histogram, co-occurrence matrix, or absolute gradient were selected, whereas none of the texture features in the run-length-matrix and AR model was selected.

DISCUSSION

In this study, we assessed potential correlation between texture features and age in sonographic images of gastrocnemius muscle

Table 4 : Selection of attributes that are relevant for discriminating three age groups. To avoid duplicates, small number of attributes were assessed (see Methods). Top 10 parameters by three evaluating methods are shown

	Age (mean, range)	Woman/man ($P=0.3$: Chi-square)
Group 1 (young) N=14	27.8 (21-42)	8/6
Group 2 (mid-age) N=14	61.4 (47-68)	6/8
Group 3 (elderly) N=14	79.2 (71-88)	10/4

Class of texture parameter and number of features	Correlation Ranking Filter	OneR feature evaluator
Histogram (1) N=9	3	4
Co-occurrence matrix (2) N=11	3	4
Run-length matrix (3) N=5	0	0
Absolute gradient (4) N=5	3	2
AR model (5) N=5	0	0
Wavelet (6) N=4	1	0

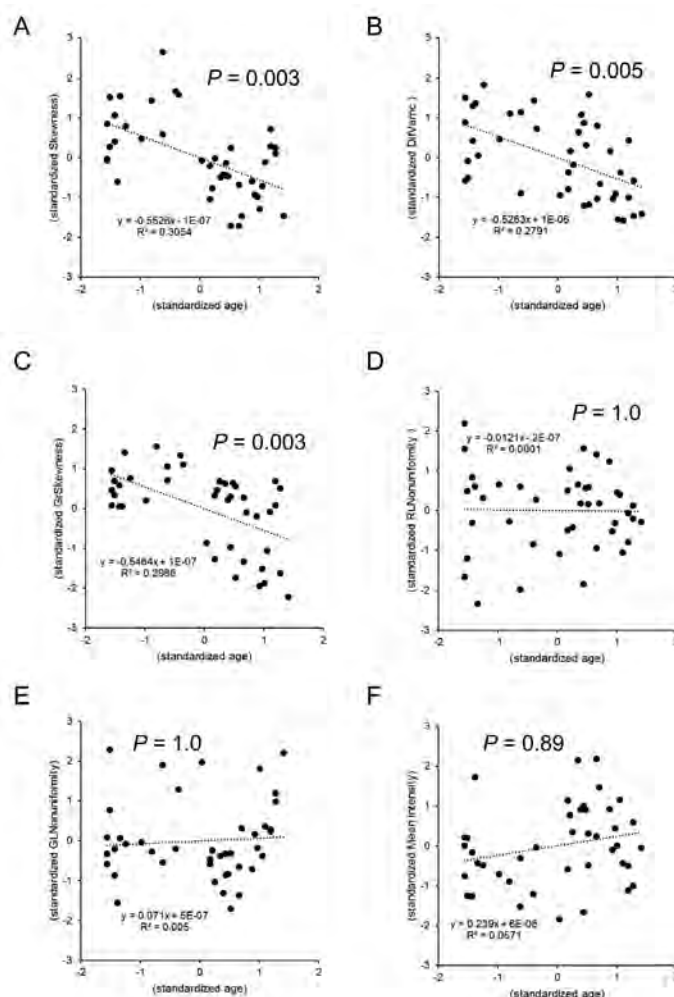


Figure 3 : Correlations between the standardized age and standardized representative texture parameters. Significant correlations are present in the following texture classes : (1) histogram (Panel A), (2) co-occurrence matrix (Panel B), and (3) absolute matrix (Panel C). No correlation was present in the parameters in the run-length matrix class (Panels D-E) and the mean signal intensity (the histogram-related class, Panel F).

DifVarnc = difference variance [Co-occurrence matrix]

GrSkewness = skewness [Absolute gradient]

RLNonuniformity = run-length nonuniformity (horizontal) [Run-length matrix]

GLNonuniformity = grey-level nonuniformity (horizontal) [Run-length matrix]

in normal subjects. We showed that there was significant difference of age-dependency among the classes of texture features. Notably, none of the texture features belonging to run-length matrix and AR model had age-dependency.

Characteristics of different texture classes

Texture features are derived from the information that are contained in the pixels of the image structure. These features are grouped into six different categories, that are discussed below. More detailed description by the developers of texture software is available (7). (1) First-order statistics are derived from the histogram of pixel intensities. Features such as the mean value, dispersion, asymmetry and sharpness are calculated. (2) A co-occurrence matrix or co-occurrence distribution is a matrix that is defined over an image to be the distribution of co-occurring grayscale pixel values at a given offset. In MaZda software, the distances of the two pixels of 1, 2, 3, 4, and 5 with angles of 0, 45°, 90°, and 135° were considered. (3) Run-length matrix-related features are calculated from a run-length matrix that is defined as the number of runs with pixels of gray level and run length. (4) Absolute gradient. The gradient of an image measures the spatial variation in grey-level values across the image. This method evaluates the relationship of variations in grey-level intensity values across neighboring pixels. (5) The AR model assumes a local interaction between image pixels in that pixel intensity is a weighted sum of neighboring pixel intensities. (6) The discrete wavelet transform is a linear transformation that operates on a data vector whose length is an integer power of two, transforming it into a numerically different vector of the same length. It separates data into different frequency components and studies each component with resolution matched to its scale.

Muscle texture features and gender

Several studies investigated the characteristic features of various texture parameters between genders. Molinari and colleagues compared texture features in young healthy individuals, mostly in their 20s and 30s (8). The authors reported that first-order texture features could distinguish the two genders. In addition, higher-order texture features such as Haralick, and local binary pattern features distinguished the genders. Higher echo intensity was commonly reported by the authors and previous studies (8, 9). Molinari and colleagues performed MANOVA analysis to distinguish between genders by using first order features alone and showed that medical gastrocnemius showed small canonical variables and the data from two genders were overlapping.

The data of the present study cannot be directly comparable to the previous studies due to different muscle groups and age distributions. Due to the large number of texture parameters, we have set the significance of the *P* value to 0.01, thus significant gender difference was present only 13/283 (4.6%) of the texture parameters.

Texture features and age

With aging, a number of changes in skeletal muscles become obvious, most notable in decline of muscle volume as shown by muscle CT (10). Elderly age is associated with decrease in subcutaneous fat (parallel to the loss of lean body mass) and the emergence of ectopic fat in muscle and other organs (11). To reflect both the quantitative and qualitative changes, skeletal muscles in the elderly show characteristic imaging features. Recently, Watanabe and colleagues reported correlations between physical characteristics (age, height, weight, body mass index, muscle strength) and several texture features (mean, skewness, kurtosis, inverse difference moment, angular second moment, and sum of entropy) in healthy adults (12). Our study is in line with the study by Watanabe and colleagues to show age-dependency

in some of the texture features. Our data indicated that women had more age dependency in their muscle texture features due to some potential reasons. First, our subjects were not equally distributed. The number of women were more than that of men, as well as more women in the oldest subjects. This difference in gender could be the reason why men showed age-dependency in texture features.

Clinical indication

This study is relevant for clinical settings. Given the recent advent of radiomics that utilizes quantitative imaging features including texture features in oncology and related fields (5, 13), there would be little doubt that this methodology of quantitative imaging analysis can be applicable to neuromuscular ultrasound. Indeed, there have been several studies to assess the texture characteristics of skeletal muscles (6, 12, 14, 8, 15-17). Among these, texture analysis of muscle ultrasound was reported to be useful in identifying the underlying etiology (i.e., myogenic vs. neurogenic in nature) (6) and in being potentially utilized as a disease biomarker, such as in amyotrophic lateral sclerosis (17). However, before reliably using muscle texture features in any clinical settings, these should be carefully assessed in the confounding factors, such as gender and aging. Watanabe and colleagues recently showed that there was indeed aging effects in the muscle texture features, although they analyzed only 6 texture features (12). Our study is in agreement with the study by Watanabe and colleagues and further extended the classes of texture features.

Limitations

As mentioned earlier, this study has limitations. First, the number of the subjects were not large. The gender was not equally distributed, largely due to smaller number of elderly men. Also, only one muscle was tested, such that generalization of the present data was difficult to be drawn. Still the authors are not aware of a study to assess a large number of texture features on their age-dependency. Second, analysis using grayscale could be influenced by system setups. By contrast, the calibrated muscle backscatter method was reported to have higher reliability among different ultrasound systems (18). In an uniform recording setting, however, the grayscale and the calibrated backscatter method resulted in highly linear correlation (19), which could favor the use of the more easily obtainable grayscale method. We are unable to find such correlation and comparison regarding texture features between the two recording methods.

Further study is clearly indicated on texture characteristics of other muscle groups in large number of subjects.

CONCLUSION

In conclusion, the present study assessed a large number of texture features in a wide range of age group showed age-dependency in many features. Thus, age should be taken into full account when utilizing texture features into diagnosis or disease progression in neuromuscular diseases. Of note, given the lack of age-dependency in the texture features related to run-length matrix and the AR model, these features could be employed as useful imaging markers for clinical use in a wide range of age groups.

CONFLICT OF INTEREST STATEMENT

None of the authors has conflict of interest.

REFERENCES

1. Simon NG, Noto YI, Zaidman CM : Skeletal muscle imaging in neuromuscular disease. *J Clin Neurosci* 33 : 1-10, 2016
2. Strasser EM, Draskovits T, Praschak M, Quittan M, Graf A : Association between ultrasound measurements of muscle thickness, pennation angle, echogenicity and skeletal muscle strength in the elderly. *Age (Dordr)* 35(6) : 2377-2388, 2013
3. Kassner A, Thornhill RE : Texture analysis : a review of neurologic MR imaging applications. *AJNR Am J Neuroradiol* 31(5) : 809-816, 2010
4. Hatt M, Tixier F, Pierce L, Kinahan PE, Le Rest CC, Visvikis D : Characterization of PET/CT images using texture analysis : the past, the present... any future? *Eur J Nucl Med Mol Imaging* 44(1) : 151-165, 2017
5. Kotrotsou A, Zinn PO, Colen RR : Radiomics in Brain Tumors : An Emerging Technique for Characterization of Tumor Environment. *Magn Reson Imaging Clin N Am* 24(4) : 719-729, 2016
6. Sogawa K, Nodera H, Takamatsu N, Mori A, Yamazaki H, Shimatani Y, Izumi Y, Kaji R : Neurogenic and Myogenic Diseases : Quantitative Texture Analysis of Muscle US Data for Differentiation. *Radiology* 283(2) : 492-498, 2017
7. Szczyplinski PM, Strzelecki M, Materka A, Klepaczko A : MaZda—a software package for image texture analysis. *Comput Methods Programs Biomed* 94(1) : 66-76, 2009
8. Molinari F, Caresio C, Acharya UR, Mookiah MR, Minetto MA : Advances in quantitative muscle ultrasonography using texture analysis of ultrasound images. *Ultrasound in medicine & biology* 41(9) : 2520-2532, 2015
9. Arts IM, Pillen S, Schelhaas HJ, Overeem S, Zwartz MJ : Normal values for quantitative muscle ultrasonography in adults. *Muscle Nerve* 41(1) : 32-41, 2010
10. Ogawa M, Yasuda T, Abe T : Component characteristics of thigh muscle volume in young and older healthy men. *Clin Physiol Funct Imaging* 32(2) : 89-93, 2012
11. Buch A, Carmeli E, Boker LK, Marcus Y, Shefer G, Kis O, Berner Y, Stern N : Muscle function and fat content in relation to sarcopenia, obesity and frailty of old age—An overview. *Exp Gerontol* 76 : 25-32, 2016
12. Watanabe T, Murakami H, Fukuoka D, Terabayashi N, Shin S, Yabumoto T, Ito H, Fujita H, Matsuoka T, Seishima M : Quantitative Sonographic Assessment of the Quadriceps Femoris Muscle in Healthy Japanese Adults. *Journal of ultrasound in medicine : official journal of the American Institute of Ultrasound in Medicine* 36(7) : 1383-1395, 2017
13. Larue RT, Defraene G, De Ruysscher D, Lambin P, van Elmpt W : Quantitative radiomics studies for tissue characterization : a review of technology and methodological procedures. *Br J Radiol* 90(1070) : 20160665, 2017
14. König T, Steffen J, Rak M, Neumann G, von Rohden L, Tonnie KD : Ultrasound texture-based CAD system for detecting neuromuscular diseases. *Int J Comput Assist Radiol Surg* 10(9) : 1493-1503, 2015
15. da Silva Pereira Junior N, da Matta TT, Alvarenga AV, de Albuquerque Pereira WC, de Oliveira LF : Reliability of ultrasound texture measures of Biceps Brachialis and Gastrocnemius Lateralis muscles' images. *Clin Physiol Funct Imaging* 37(1) : 84-88, 2017
16. Matta TTD, Pereira WCA, Radaelli R, Pinto RS, Oliveira LF : Texture analysis of ultrasound images is a sensitive method to follow-up muscle damage induced by eccentric exercise. *Clin Physiol Funct Imaging* : 2017
17. Martinez-Paya JJ, Rios-Diaz J, Del Bano-Aledo ME, Tembl-Ferrairo JI, Vazquez-Costa JF, Medina-Mirapeix F : Quantitative Muscle Ultrasonography Using Textural Analysis in Amyotrophic Lateral Sclerosis. *Ultrason Imaging* : 16173461 7711370, 2017
18. Zaidman CM, Holland MR, Hughes MS : Quantitative ultrasound of skeletal muscle : reliable measurements of calibrated muscle backscatter from different ultrasound systems. *Ultrasound Med Biol* 38(9) : 1618-1625, 2012
19. Shklyar I, Geisbush TR, Mijalovic AS, Pasternak A, Darras BT, Wu JS, Rutkove SB, Zaidman CM : Quantitative muscle ultrasound in Duchenne muscular dystrophy : a comparison of techniques. *Muscle Nerve* 51(2) : 207-213, 2015